ESRF	**Experiment title:** Swelling/Deswelling Kinetics of Temperature-Sensitive PNIPAM Microgels in Mixed Solvents	**Experiment number**: SC-3475
Beamline: ID-02	**Date of experiment**: from: 23.11.2012 to: 26.11.2012	**Date of report**: 23/07/2013
Shifts: 9	**Local contact(s)**: Dr. Gudrun Lotze	*Received at ESRF:*

Names and affiliations of applicants (* indicates experimentalists):

Dersy Lugo*; Christine Scherzinger*, Cornelius Hofzumahaus*, Walter Richtering (Institute of Physical Chemistry, RWTH Aachen,Landoltweg 2, D-52056 Aachen, Germany)

Report:

PNIPAM is one of the most widely studied water-swellable microgel system. It is a thermosensitive microgel and becomes insoluble in aqueous solution at 32 °C.[1] This temperature is known as the volume phase transition temperature (VPTT). The PNIPAM microgels do not only exhibit a well-defined temperature-induced phase transition in aqueous media, but also a so-called cononsolvency effect.[2] This term describes the phenomenon that the polymer is insoluble in a certain concentration range of solvent mixtures, while being soluble in the pure solvents. Previous works [2-3] showed that the PNIPAM microgel particles deswell to a minimum size upon the addition of alcohols and then, reswell again as the alcohol-rich region is approached.

These stimuli-responsive properties of the microgels make them special materials for applications in many fields, especially in the industrial and biomedicals areas Therefore, their properties has been widely studied, but all these studies have been focused to investigate the size, shape, morphology, composition and VPTT of the microgel particles and relatively few research has been reported on their volume phase transition (VPT) kinetics by means of the stopped flow technique[4] or nanosecond laser-induced temperature-jump technique[5] .

To the best of our knowledge, the swelling/deswelling kinetics of microgels induced by a change of solvent composition has not been reported yet, Therefore, in this contribution we have exploited the cononsolvency effect to study the collapsed kinetics of PNIPAM microgels by means of the stopped flow-SAXS technique.

The solvent exchange kinetics in PNIPAM microgels implicate a different and more complicated process for the VPT of microgels that those induced by temperature- or pH-jump reported in the literature,[4,5] since in the cononsolvency phenomenon the volume transition of the microgel particles requires first that a co-nonsolvent (*e.g.* methanol) penetrates into the microgel and, then, when sufficient solvent has been exchanged, the solvent mixture is expelled when the particle shrinks. Thus, a coupled mass-transport is involved in the cononsolvency process, in which the mass transport of each solvent (*e.g.* methanol and water) is different as compared to the transport of protons used in pH-jump experiments.[5]

In addition, exploiting the cononsolvency effect will not only allow studying both deswelling and swelling with the same system but also by different routes. *E.g.* particles swollen either in water (H_2O) or in methanol (MeOH) can be completely collapsed by adding either methanol or water, respectively.

We have used PNIPAM microgels of 5 different sizes in the range of 800 nm – 2 µm dispersed in H_2O and in MeOH in our time-resolved SAXS experiment on the beamline ID02. The measurements were made at a temperature of 10 °C below the VPTT of the particles in H_2O (32°C) and the final concentration of the PNIPAM microgel in the desired final H_2O/MeOH solvent composition was set to 0.4 wt%. In this experiment, we focused mostly in the solvent exchange collapse transition kinetics starting from different initial states (starting with dispersions of PNIPAM in pure H_2O or in pure MeOH) to reach the same final state (dispersions of PNIPAM in a mole fraction of methanol (x_{MeOH}) of 0.20). All measurements were made at a wavelength of 1Å . The samples were measured at three different detector distances (3m, 8m, and 10m). Additionally, we performed static measurements in a flow-through cell to determine the initial and final state of our particles at 10 °C.

PNIPAM dispersions in pure solvent (either H_2O or MeOH), H_2O, and MeOH were injected into the stopped-flow apparatus. A PNIPAM dispersion and its contrarion solvent, i.e. a PNIPAM dispersion in pure H_2O was mixed turbulently with MeOH and vice versa, were injected for 50ms continously into the flow path of the stopped-flow device corresponding to a steady state condition. X-ray data acquistion was triggered directly before those 50ms. The sample age of the mixed solution during this steady state was mainly determined by the necessary time to flow from the mixer inside the stopped flow device to the point of X-ray exposure. This initial dead time was 3 ms. The effective exposure time for each frame was 1.5 ms meaning that each scattering curve was integrated over 1.5 ms. Consequently, the first scattering curve describes the kinetic at a point in time of 3.75ms. The minimum detector readout time during the experiment was 320 ms, hence a stroboscopic data strategy was necessarily applied to access points in time well before 320ms. This was achieved by varying the first dead time before the first X-ray exposure, i.e. a delay time of 50 ms, 55 ms, 60 ms, 70ms etc. was introduced.

Each mixing experiment was repeated with first acquisition delayed 50, 55, 60, 70 ms, etc. Each acquisition was repeated three times to improve the statistics and to verify the reproducibility. Subsequently, all curves were averaged for each point in time. Model fitting has been carried out using the NIST SANS analysis package[6], a form factor for polydisperse microgels developed by Stieger et al.[7] and for polydisperse core-shell microgels developed by Berndt et al.[8]

As an example, we present here the results for the biggest particle used on this experiment in the solvent composition jump from pure MeOH to x_{MeOH} = 0.20. Figure 1 shows a time series of SAXS curves over the full range of the measured times, in which many form factors minima are observed. As it can be seen on the first two acquisitions, it is not possible to observe the first form factor minimum ($q_{min,1}$) due to the fact that this minimum is out of the q range of the ID02. With time the first form factor minimum appears and shifts to higher q regions.

More oscillations at the higher q region are as well evident, indicating shrinking and a narrower size indicating shrinking and a narrower size distribution of the particles with time. In Figure 1, curves were

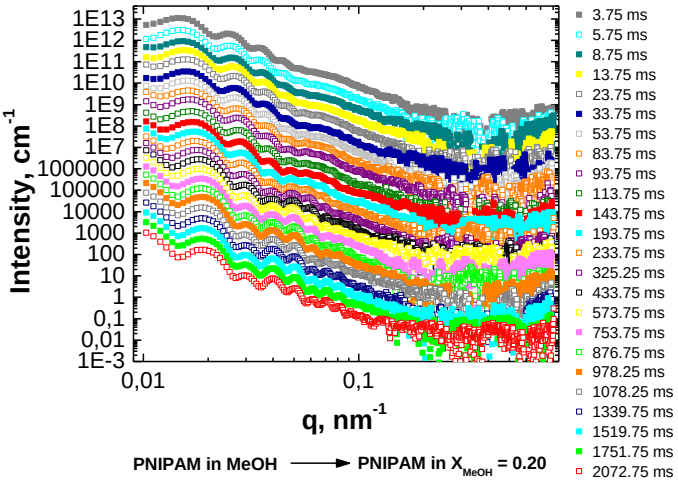

Figure 1. Radial averaged SAXS diffraction pattern for the biggest PNIPAM in the solvent composition jump from pure MeOH to x_{MeOH} = 0.20. Times were corrected for the 50ms offset.

vertically shifted to higher intensities by multiplication for better visibility.

The radius of the microgel was determined from the position of $q_{min,1}$ and with this information the evolution of the microgel size with time was derived (Fig. 2). The position of $q_{min,1}$ provides information about the radius of collapsed microgel particles, as they behave similar as hard spheres at this state. In the case of swollen microgel particles, the position of $q_{min,1}$ provides information about the radius from the center of the particle to the half-width of its fuzziness (see Fig. 1 on reference [7]). Since swollen microgels exhibit an inhomogeneous density with a cross-linking density decreasing from the center towards the periphery and this leads to a fuzziness of the particle surface.

In Figure 2 the evolution of the microgel size with time is plotted for the biggest PNIPAM microgel for two solvent composition jumps starting from different initial states to reach the identical final state.

It can be observed that the equilibrium radius is similar in both cases, as expected. This minimum radius is in the order of 309 nm (similar to the microgel radius at x_{MeOH} = 0.20 obtained by static light scattering measurements performed at 20 °C ($R_{qmin.1} \approx 307$ nm)). It seems that the temperature inside the cuvette increases by 10°C, due to the heat released by mixing H_2O and MeOH in order to obtain a final solvent composition of x_{MeOH} = 0.20, as it has been predicted theoretically assuming an adiabatic process without friction and verified experimentally by measuring the temperature inside the stopped flow cuvette during the kinetics measurements with a cable sensor Pt100 and recording the temperature with time.

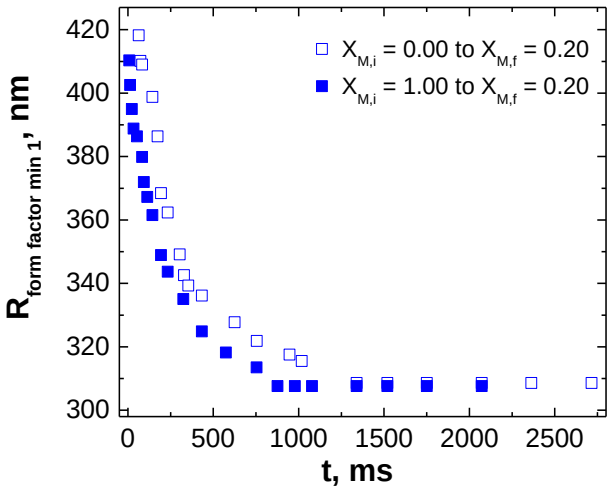

Figure 2. Evolution of the microgel size with time after two different solvent composition jumps.

Another important feature of this plot is that collapse transition kinetics of PNIPAM induced by adding MeOH to the aqueous dispersion of the microgel is slower than that induced by the addition of H_2O to the dispersion of PNIPAM in pure MeOH.

At the early stages of the collapse transition during the solvent exchange, one might expect that microgel volume transitions would occur first at the microgel periphery and proceed towards the interior. That would lead to the formation of a desolvated shell of polymer surrounding a solvated core. The hydrophobicity of this skin layer tunes the diffusion rate of the solvent from the shell and subsequently from the particle interior. Then further deswelling occurs by a thickening of the desolvated layer and a decrease of the swollen core until an equilibrium state is reached where the microgel particle exhibits a homogeneous density profile similar to the hard spheres.

According to the explanation given above, we could fit the form factor curves at the final state with a model for spheres with homogeneous density. But the curves corresponding to the points in times before the equilibrium state could not be very well described with a core-shell form factor model. We have found a very good agreement if we assume a bimodal dispersion containing spheres and core-shell spheres with homogeneous density and the shell becomes thicker and thicker with time. Figure 3 shows scattering curves for the biggest PNIPAM in the solvent composition jump from pure MeOH to x_{MeOH} = 0.20 at a time before the equilibrium state (≈ 193.75 ms) and at the equilibrium state (≈ 2072.75 ms). The cartoons in the plots represent the morphology of the PNIPAM particles at the corresponding time. As can be seen, the cartoon at 193.75 ms corresponds to the existence of two kind of morphologies of the PNIPAM particles with different sizes (spheres and core-shell spheres with homogeneous density). The drawback of the assumption of a

bimodal dispersion is that the radius of the homogeneous spheres is significantly bigger than the radius estimated from the position of $q_{min,1}$, and moreover, to the core-shell spheres radius. This preliminary analysis indicates that the system is more complicated than expected and therefore we will try as a next step to fit the curves with other core shell spheres form factor. In the first model a polydisperse shell will be assumed [6]; in the second model a shell with decaying density profile[9] will be assumed; and in the third model an asymmetric interface between the core and the shell it will be assumed[10].

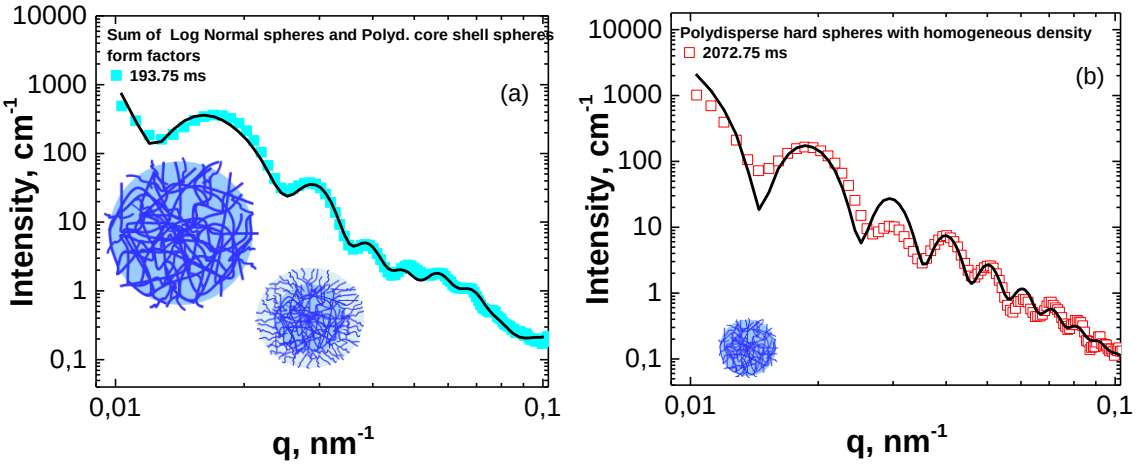

Figure 3. Radial averaged SAXS diffraction pattern for the biggest PNIPAM in the solvent composition jump from pure MeOH to x_{MeOH} = 0.20: (a) before the final state (t = 193.75 ms); (b) at the final state (t = 2072.75 ms). The cartoons

A similar behaviour was observed for the other PNIPAM microgels, in which a faster response rate of the collapse transtion kinetics was observed by decreasing the particle size, in concordance with the Tanaka-Fillmore Theory[11].

In summary, we were able to obtain high quality data observing for the first time to our best knowledge with time-resolved SAXS the solvent exchange kinetics collapse transition in PNIPAM microgels. We will now focus on the modeling of this data and explore different model approaches to describe the internal structure changes of the polymer network induced by cononsolvency effect.

References

[1] R.H. Pelton, P. Chibante, *Colloids Surf.* **1986**,*120*, 247-256.

[2] F. M. Winnik, H. Ringsdorf, J. Venzmer, *Macromolecules* **1990**, *23*, 2415-2416; F. M. Winnik, M. F. Ottaviani, S. H. Bossmann, M. Garcia-Garibay, N. J. Turro, *Macromolecules* **1992**, *25*, 6007-6017.

[3] H. M. Crowther, B. Vincent, *Colloid Polym Sci* **1998**, *276*, 46-51; G. Zhang, C. Wu, *J. Am. Chem. Soc.* **2001,** *123*, 1376-1380; C. Scherzinger, P. Lindner, M. Keerl, W. Richtering, *Macromolecules* **2010**, *43*, 6829-6833.

[4] J. Wang, D. Gan, L. A. Lyon, M. A. El-Sayed, *J. Am. Chem. Soc.*, **2001**, *123*, 11284-11289.

[5] D. Dupin, J. Rosselgong, S. P. Armes, A. F. Routh, *Langmuir*, **2007**, *23*, 4035-4041; J. Yin, D. Dupin, J. Li, S. P. Armes, S. Liu, *Langmuir*, **2008**, *24*, 9334-94340.

[6] S. R. Kline, *J. Appl. Cryst.* **2006**, *39*, 895-900.

[7] M.Stieger, W. Richtering, J.S. Pedersen, P. Lindner, *J. Chem. Phys*. **2004**, *120*, 6197-6206.

[8] I. Berndt,; J. S. Pedersen, W. Richtering, *J. Am. Chem. Soc.* **2005**, 127, 9372–9373.

[9] C. M. Wijmans, E. B. Zhulina, Macromolecules 1993, 26, 7214-7224.

[10] I. Berndt,; J. S. Pedersen, W. Richtering, *Angew. Chem., Int. Ed.* **2006**, 45, 1737–1741.

[11] Tanaka T.; Fillmore D. J. *J. Chem. Phys.* **1979**, *70*, 1214-1218.